

## Effects of Varying Ramp Rate and Amount of ES

David Gonsoulin\*, Gokhan Ozkhan, Behnaz Papari, Chris S. Edrington

*Florida State University*

\* Corresponding Author. Email: dg11g@fsu.edu

### Synopsis

This paper will address the usage of combined power and energy management control layers to systematically study the effect of intelligently varying generator ramp rates and its impact on required energy storage in the presence of mission load profiles. The work will utilize a developed notional 4-zone representation of a destroyer-class ship in which there is an energy management layer (composed of a distributed model predictive control) and a power management layer (composed of a distributed droop control). The work will analyze conditions in which the ship must fire a pulsed-power load. The effect of the energy management to leverage available energy storage versus allowing generator ramp-rates to exceed standards in the presences of the aforementioned conditions will be studied to illustrate how the consideration of system-level control is critical in the design cycle.

*Keywords:* Distributed control, Energy Management, and energy storage

### 1. Introduction:

The drive to create a more autonomous ship power system is inextricably linked to distributed control. Distributed control, enabled by high-speed networked communication and power electronics, provides a systematic way of increasing autonomy while simultaneously addressing system efficiency and resiliency in meeting mission loads.

The control structure consists of primarily three critical layers: energy management, power management, and device level control. The energy management is the focus of this paper. The power management layer, consisting of an advanced control framework, enabled via networked communication, provides for appropriate sharing of power among various devices while simultaneously meeting bus voltage requirements and providing stability to the electrical system. The energy management layer optimizes over a time horizon to provide appropriate resource allocation to meet mission objectives in the presence of associated mission profiles and electrical apparatus constraints, with respect to competing objectives such as: system efficiency, resiliency, quality of service, and load prioritization.

Ship system design is a critical topic in helping to meet the US Navy's desire to project force with more efficient and resilient vessels that are fitted with a variety of high-ramp rate, nonlinear loads intended to achieve mission objectives. Although current design cycles consider that there will be some form of control, there has yet been research to evolve any systematic integration of power and energy management in the overall design process. However, system-level control is critical in leveraging all available resources: generation, storage, and load shedding in order to meet mission demand. To date, there are no systematic studies that illustrate the effect of energy management on system design. Also, there has not been any systematic studies of how energy management enabled via distributed control can affect a potential reduction in storage via leveraging of all distributed energy resources aboard ship.

### 2. Energy Management Methodology

The Energy Management uses a hybrid method, which is a combination of two control algorithms to achieve the control objective: a DMPC algorithm and an algebraic consensus algorithm. The two algorithms are utilized at different periods to achieve different objectives. The objectives of the Energy Management are to: a) ensure the power ramp rate needed by the loads is met and b) ensure that the final state of charge (SOC) of the energy storages (ES) equal a predefined SOC reference. The power ramp rate fulfillment and the desired SOC can be formulated as shown in (1) and (2), respectively. In this paper, the DMPC algorithm will be developed to fulfill the objective formulated in (2) while the algebraic consensus algorithm is developed to fulfill the objective formulated in (1).

$$\sum_{j=1}^2 r_{Lj} = \sum_{i=1}^2 r_{GENi} + \sum_{i=1}^2 r_{ESi} \tag{1}$$

$$E_{ESi}^* = E_{ESi} \tag{2}$$

Based on the motivation of this work described in the Introduction section, the ramp rate constraints in generator devices are the main concern. These constraints can be seen in (3). The proposed algorithm for the EM aims to ensure that the ramp rate constraints of the generators are not violated.

$$r_{ES}^{min} = r_{GEN}^{min} - r_L \leq r_{ES} \leq r_{ES}^{max} = r_{GEN}^{max} - r_L \tag{3}$$

The flowchart of the proposed method can be illustrated in Figure 1. The next section will detail the method.

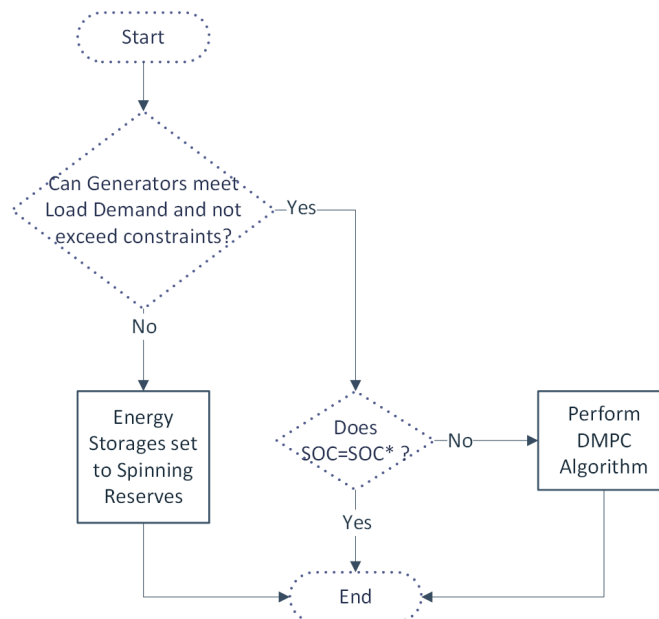


Figure 1. Energy Management Control Algorithm. SOC\* is the desired state of charge of an energy storage.

### 2.1.1. DMPC with ADMM

To start, a formulation of the model used for the MPC is needed. The ES are modeled as

$$E_{ESi,k+1} = E_{ESi,k} + TP_{ESi,k} \tag{4}$$

Where

$$P_{ESi,k+1} = P_{ESi,k} + Tr_{ESi,k} \tag{5}$$

Here, k represents a discrete time, T is the sampling time,  $E_{ESi,k+1}$  is the energy of ES i at time k+1,  $P_{ESi,k+1}$  is the power of ES i at time k+1, and  $r_{ESi,k}$  is the ramp rate of ES i at time k.

Augmentation of the original ES model allows a transparent way in the MPC control realization for meeting the control objective. Therefore, an augmented model for the ES will be formulated as follows: Define  $\Delta E_{ES,k}$  and  $\Delta P_{ES,k}$  as

$$\Delta E_{ES,k} = E_{ES,k} - E_{ES,k-1} \tag{6}$$

$$\Delta P_{ES,k} = P_{ES,k} - P_{ES,k-1} = T r_{ES,k-1} \tag{7}$$

If (6) and (7) are substituted into (4), the resultant equation is below.

$$\Delta E_{ES,k+1} = \Delta E_{ES,k} + T \Delta P_{ES,k}. \tag{8}$$

By defining  $x_k = [\Delta E_{ESi,k} \quad E_{ESi,k}]^T$  as the augmented state and combining (4) and (5) with (8), the final state space equation is found.

$$x_{k+1} = Ax_k + B \Delta P_{ESi,k} \tag{9}$$

Where

$$A = \begin{bmatrix} 1 & 0 \\ 1 & 1 \end{bmatrix}, B = \begin{bmatrix} T \\ 0 \end{bmatrix}, C = [0 \quad 1] \tag{10}$$

Next, the predictive control formulation and solution is derived.

$$\bar{E}_{ESi} = G x_{ESi,k} + \Phi \bar{\Delta P}_{ESi} \tag{11}$$

Where

$$\begin{aligned} \bar{E}_{ESi} &= [E_{ESi,k+1}, E_{ESi,k+2}, \dots, E_{ESi,k+N_p-1}]^T \\ \bar{\Delta P}_{ESi} &= [\Delta P_{ESi,k+1}, \Delta P_{ESi,k+2}, \dots, \Delta P_{ESi,k+N_p-1}]^T \\ G &= \begin{bmatrix} CA \\ CA^2 \\ \vdots \\ CA^{N_p} \end{bmatrix}, \Phi = \begin{bmatrix} CB & 0 & \dots & 0 \\ CAB & CB & \dots & 0 \\ \vdots & \vdots & \ddots & \vdots \\ CA^{N_p-1}B & CA^{N_p-2}B & \dots & CA^{N_p-N_c}B \end{bmatrix} \end{aligned} \tag{12}$$

The cost function is shown as

$$J(\bar{\Delta P}_{ESi}) = (\bar{E}_{ESi}^* - \bar{E}_{ESi})^T (\bar{E}_{ESi}^* - \bar{E}_{ESi}) + \bar{\Delta P}_{ESi}^T I_{N_c \times N_c} \bar{\Delta P}_{ESi} \tag{13}$$

Where  $\bar{E}_{ES}^* = [E_{ES}^*]_{2N_p \times 1}$ . The cost function is subject to the following constraints

$$A_{ieq} \bar{\Delta P}_{ESi} \leq b_{ieq} \tag{14}$$

Where

$$\begin{aligned} A_{ieq} &= \begin{bmatrix} 1 & 0 \\ 0 & 1 \end{bmatrix} \\ b_{ieq} &= T [-r_{ES}^{min} \quad r_{ES}^{max}]^T \end{aligned} \tag{15}$$

In order to ensure that the ES provide power when the ramp rate demand of the loads exceeds that of the generator constraints, the following augmentation of  $r_{ES}^{min}$  and  $r_{ES}^{max}$  is done.

$$\begin{aligned} r_{ES}^{min} &= -r_{GEN}^{min} - r_{Load} \\ r_{ES}^{max} &= r_{GEN}^{max} - r_{Load} \end{aligned} \tag{16}$$

By minimizing the cost function subject to these constraints, an optimal power reference is chosen to apply to the ES for the next time step that achieves the desired objective.

Using ADMM, the cost function  $J$  can be formulated as follows:

$$\min_x \left( \frac{1}{2} \Delta \bar{P}_{ESi}^T M \Delta \bar{P}_{ESi} + \Delta \bar{P}_{ESi}^T F + \|x - z + u\|_2^2 \right) \tag{17}$$

The minimization of this cost function results in the initial optimal control input of  $\Delta \bar{P}_{ESi}$ .

Next, the integration of the ADMM algorithm and the above MPC formulation will be introduced. This algorithm is performed on each controller. To start, an overview of the ADMM algorithm is helpful. Figure 2 shows a diagram of how the steps are implemented in each distributed control agent.

1. Start
2. Initialize  $\lambda = 0, z = 0$
3. Repeat
  - a.  $x^{k+1} = \operatorname{argmin}_x J(x_i, z^k, u^k)$
  - b. Communicate with neighbors  $j (j \in N_i)$  to exchange  $x^{k+1}$
  - c.  $z^{k+1} = \frac{1}{N_{i+1}} \sum_{j \in N_i \cup i} x_j^{k+1}$
  - d.  $u_i^{k+1} = u_i^k + \rho(x_i^{k+1} - z_i^{k+1})$
4. Check stopping criteria (maximum iteration or minimum residuals)

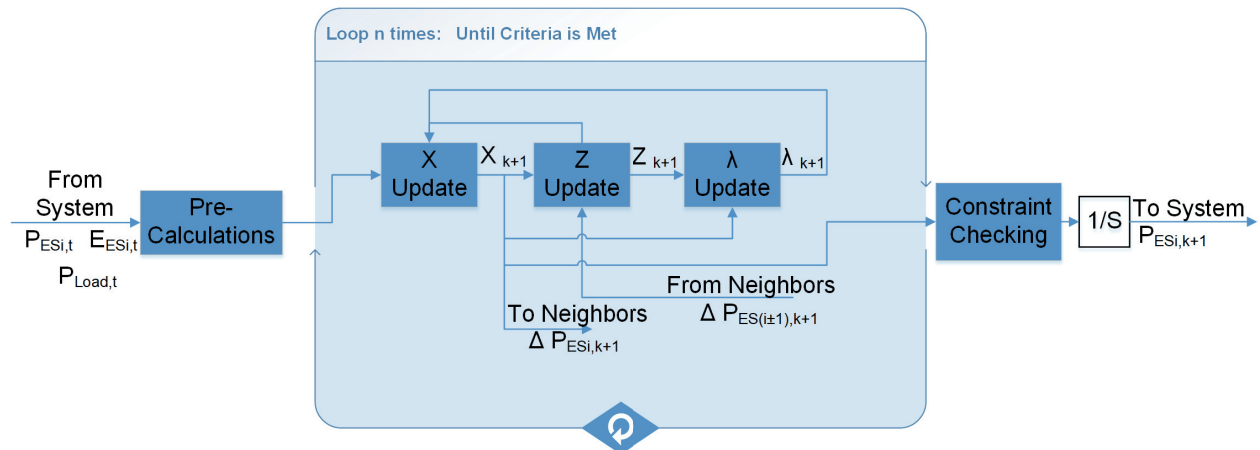


Figure 2. MPC with ADMM Algorithm

Within the repeat stage, step a. is called the x-update. The equation used for this step is calculated as follows. First, perform the partial differential equation with respect to  $x (x = \Delta \bar{P}_{ESi})$ .

$$\frac{\partial J}{\partial \Delta \bar{P}_{ESi}} = \frac{1}{2} \Delta \bar{P}_{ESi}^T M \Delta \bar{P}_{ESi} + \Delta \bar{P}_{ESi}^T F + \|x - z + u\|_2^2 = 0 \tag{18}$$

Where

$$\begin{aligned} M &= 2(\Phi^T \Phi + I_{N_c \times N_c}) \\ F &= -2\Phi^T (\bar{E}_{ESi}^{ref} - Gx_k) \end{aligned} \tag{19}$$

(18) results in the following equation which gives the optimal control setpoint for a single ES based on the local information. Here,  $\rho$  is a weighting variable.

$$\Delta \bar{P}_{ESi} = (M + \rho)^{-1} (-F + \rho z - \rho u) \tag{20}$$

(20) gives the  $x^{k+1}$  solution that is used in step 3-a of the ADMM algorithm. Next, each controller will communicate the  $x^{k+1}$  value calculated with its neighbors (step 3b). Before step 3c is calculated, some additions to the algorithm needed to be made. In the current state of the algorithm (shown above), the controllers reach a consensus on the  $x$  value, which is  $\Delta P_{ES}$  in this case. Each ES can have a different desired SOC and a different initial condition. If the algorithm was to reach a consensus on  $\Delta P_{ES}$ , there the ES would not reach their desired SOC at the same time. Specifically, the goal is to reach a consensus on the state of charge; therefore, the  $z$  and  $u$  updates must be augmented in a way to achieve this objective. Prior to the  $z$  update, the SOC must be found. This is done using

$$SOC_{\%,i} = E_{ESi,k} + T \left( P_{ESi,k} + T(\Delta \bar{P}_{ESi,k+1}) \right) \tag{21}$$

Based on the  $SOC_{\%,i}$  for the agent and its neighbors, the  $z$  update can be calculated by finding the average. Step 3d is the lagrange multiplier ( $\lambda$ ) update, which is used to determine whether or not a consensus between controllers was reached. In order to use  $z$  update,  $x$  must be a  $SOC_{\%,i}$  value calculated using (21).

Once the maximum number of iterations is reached or the minimum residual is met, the method performs the final step of constraint checking. To ensure that the collective actions of the ES do not exceed the collective generators' ramp rate constraints, the following constraint checking was employed. First, the sum of  $\Delta \bar{P}_{ESi}$  for all the ES is found using (22).

$$\Delta \bar{P}_{ES \text{ total}} = \sum_{i=1}^N |\Delta \bar{P}_{ESi}| \tag{22}$$

Next, a ratio specific to each agent is found using (23).

$$\psi_i = \frac{\Delta \bar{P}_{ESi}}{\Delta \bar{P}_{ES \text{ total}}} \tag{23}$$

Next, the total ramp rate limitations of all the generators is augmented using this ratio.

$$\begin{aligned} r_{aug_{ESi}}^{max} &= \psi_i * r_{Gens}^{max} \\ r_{aug_{ESi}}^{min} &= \psi_i * r_{Gens}^{min} \end{aligned} \tag{24}$$

where  $r_{Gens}^{max}$  and  $r_{Gens}^{min}$  represent the total ramp rate limitations of all the generators combined. Next, the constraints are checked with the desired  $\Delta \bar{P}_{ESi}$ , and the final value is used as the power reference for ES  $i$ .

$$\Delta P_{ESi} = \min(r_{aug_{ESi}}^{max}, \max(r_{aug_{ESi}}^{min}, \Delta \bar{P}_{ESi})) \tag{25}$$

### 2.1.2. Spinning Reserve

While the DMPC with ADMM is used to ensure the SOC is maintained when the ES are not in use, the spinning reserve mode has the responsibility of coordinating the distributed ES when a high-power ramp rate load is activated. The control diagram is shown in Figure 3. This control allows each agent to reach an equal control input for the distributed ES.

$$P_{ES,i}^* = P_{Load,Filtered} + k \int \sum_{j=1}^{N_j} (P_{ES,i} - P_{ES,j}) \tag{26}$$

The control requires the power amount of the load to be serviced, and the power output of the agent's own ES and its neighbors. These values are used in the algorithm to provide a power setpoint for the agent's ES.

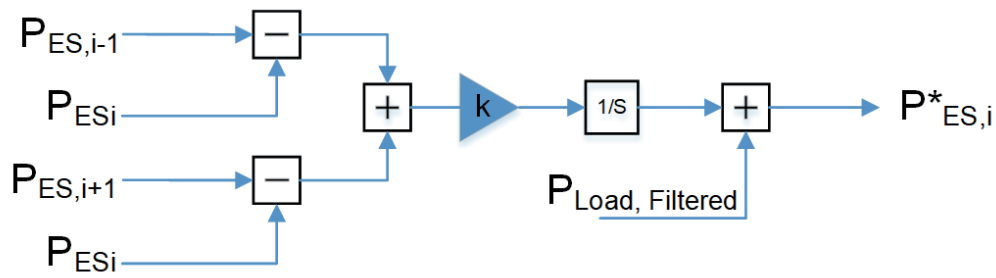


Figure 3. Spinning Reserve Algorithm

### 3. Experimental Setup

The experiment was done in the Energy Conversion and Integration Thrust lab at the Center for Advanced Power Systems. The experimental setup is shown in Figure 4.

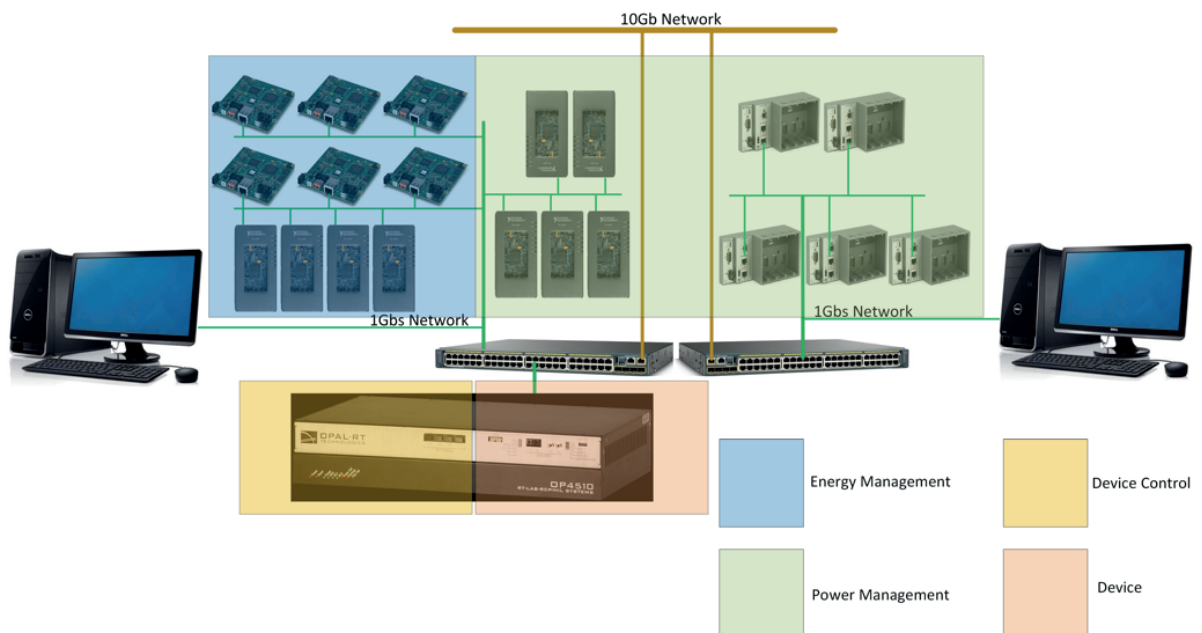


Figure 4. Experimental Setup

The main components for this experiment are the Opal RT OP4510 real time simulator, the national instruments controllers, and the Ethernet communication network. Each aspect will be described below.

The power system is shown in Figure 5; it mimics a proposed zonal power system that the Navy is moving towards. In this system, there are 3 main gas turbine generators, 2 auxiliary gas turbine generators, 5 energy storages, 2 propulsion motors, 4 AC load centers, a radar, and an electromagnetic railgun.

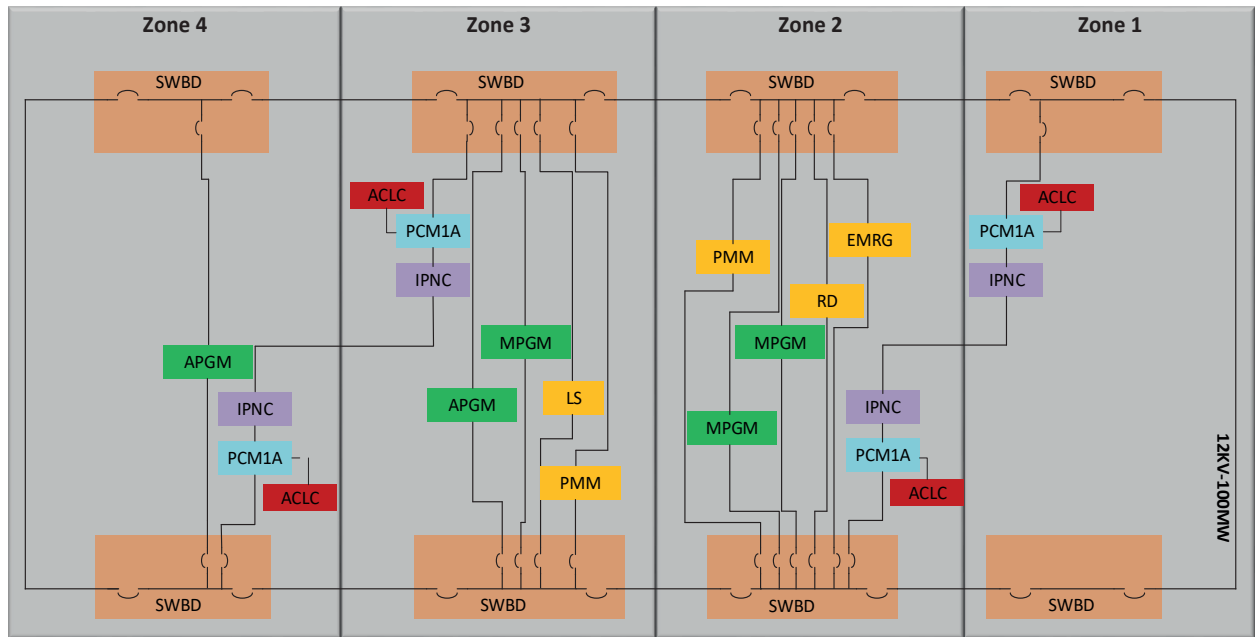


Figure 5. Power System for Experiment

This model was built in Simulink and modified to run in real time on an Opal-RT OP4510 system. The model did not contain any power electronics; it simply used controllable ideal voltage and current sources to achieve the desired sources and loads. The final configuration is shown in Figure 5 with all the switches closed. A single core was used to run the model. The model runs at a time step of 50µs. The load profile is shown in Figure 6. Relevant values for this model are shown in Table 1 and Table 2.

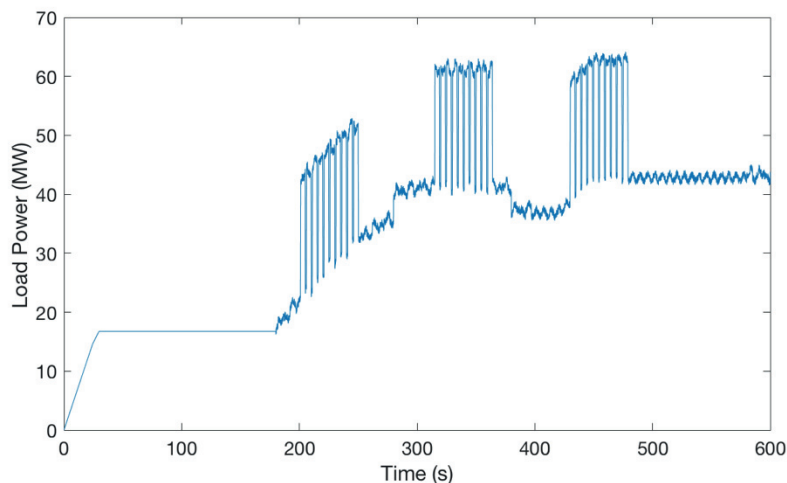


Figure 6. Load Profile

Quantity	Name	Value
Rated Main Bus Voltage	$V_{bus}^{rate}$	12 kV
Rated Power of MPGM1	$P_{MPGM1}^{rate}$	34.8 MW
Rated Power of MPGM2	$P_{MPGM2}^{rate}$	34.8 MW
Rated Power of MPGM3	$P_{MPGM3}^{rate}$	34.8 MW
Rated Power of APGM1	$P_{APGM1}^{rate}$	4.48 MW

Rated Power of APM2	$P_{APGM2}^{rate}$	4.48 MW
Rated Power of Each ES	$P_{ES}^{rate}$	5 MW
Rating limits of Each ES	$R_{ES}^{rate}$	40 MW/s
Rated Power of Each PMM	$P_{PMM}^{rate}$	36 MW
Rated Power of Each Service Load	$P_{Service}^{rate}$	5 MW
Rated Power of EMRG	$P_{EMRG}^{rate}$	20 MW
Rated Power of Laser	$P_{LS}^{rate}$	1 MW

Table 1. Ratings in System

Quantity	Name	Value
Prediction Horizon	$N_p$	100
Control Horizon	$N_c$	1

Table 2. Values used in Control

For the controllers, National Instruments RIOs were used. myRIOs, sbRIOs, and cRIOs comprised the setup and totaled to 15 controllers. For the Energy Management presented in this paper, 5 of these controllers were used to control the 5 ES. As for the remaining 10 controllers, they were used for a power management layer. All of these controllers were connected to a local Ethernet network.

There were two different communication protocols used. The UDP protocol was used between the OP4510 and all of the controllers. The RTI DDS protocol was used between the controllers to facilitate the control algorithms. A value update occurred every 1ms for both communication protocols. The values that were sent over the communication infrastructure is shown in Table 3.

Values sent:	To Opal	To Controllers
From Opal	NA	$P_{ES,i}, E_{ES,i}, P_{L,Filtered},$ Railgun Activation Signal
From Controllers	$P_{ES,i}^*$	$\Delta P_{ES,i}, P_{ES,i}, E_{ES,i}$

Table 3. Values sent over Communication Infrastructure

During each time-step for the model, the opal performed the model calculations and checked to see if there was an updated power setpoint, received via UDP from the controllers, for the ES. If there was a new setpoint, the model would be updated with the new setpoint; the OP4510 would then send a multitude of values back to the controller it received a setpoint from. When battle mode was active, a new setpoint was sent every 1ms. When recharging of the ES was active, a new setpoint was sent every 250ms.

In Table 4, the different ES sizes and generator ramp rate limitations are shown. Each ES varied in size from 70MJ to 25MJ. For each of the three different ES sizes, the maximum ramp rate per generator for the recharging sequence was varied.

70MJ per ES	50MJ per ES	25MJ per ES
1MW/s	1MW/s	1MW/s
1.5MW/s	1.5MW/s	1.5MW/s
2MW/s	2MW/s	2MW/s

Table 4. Case Studies

#### 4. Results and Discussion

The 70MJ per ES and 1MW/s per generator case will be shown as a baseline. For these settings, the high-power ramp rate load demand is met fully without reaching a 0% SOC on the ES.

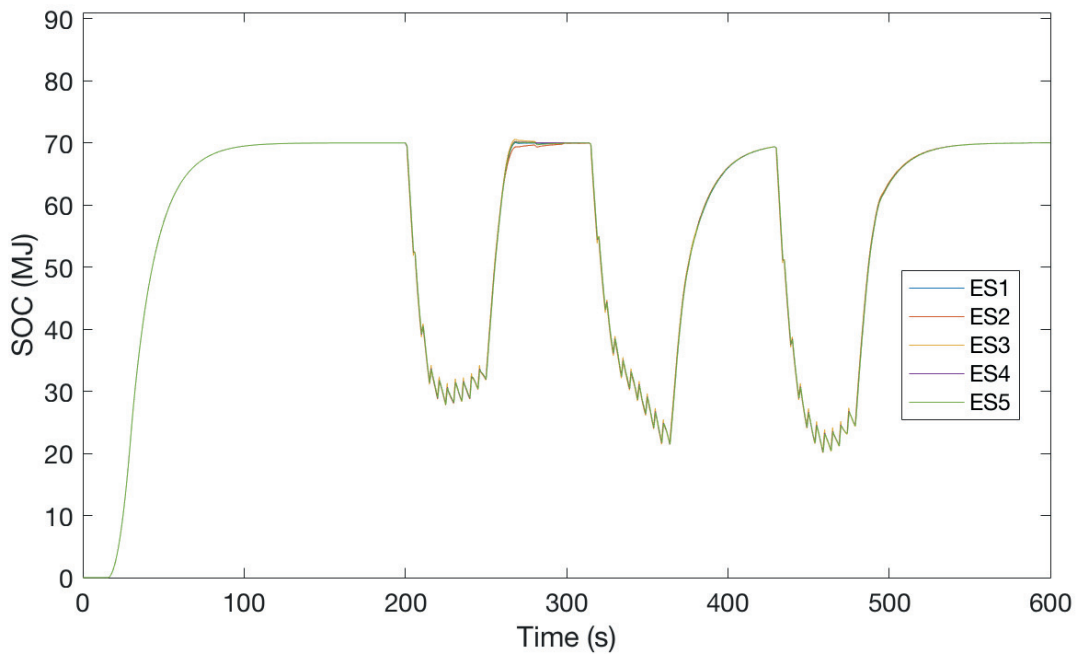


Figure 7. Energy for 70MJ per ES and 1MW/s Ramp Rate per Gen

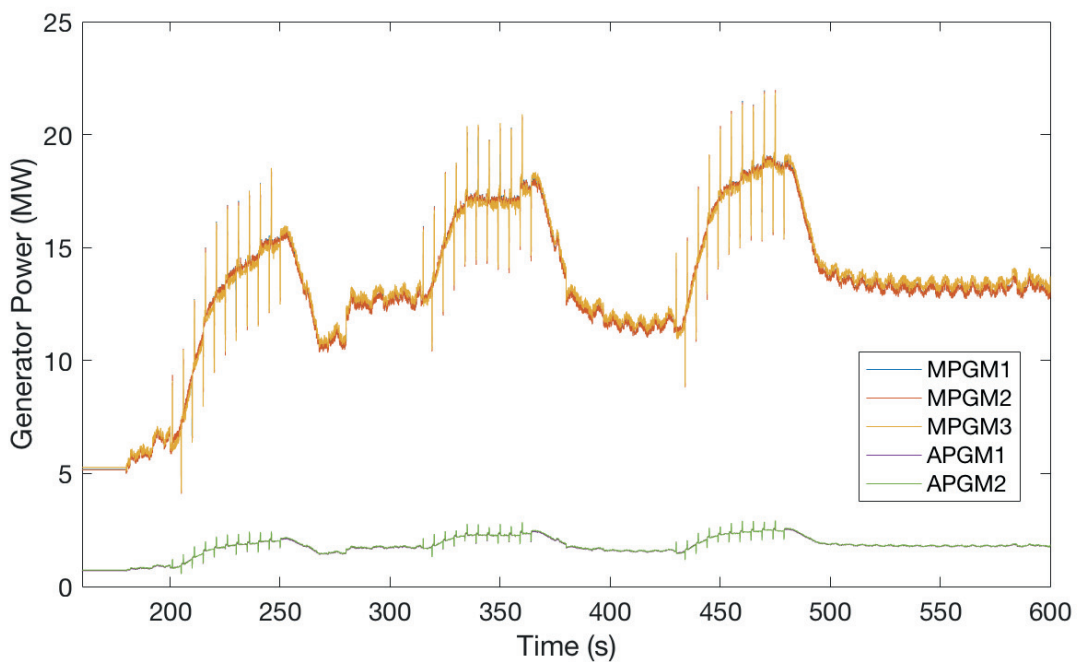


Figure 8. Power for Generators for 70MJ per ES and 1MW/s Ramp Rate per Gen

When looking at the 50MJ per ES case, issues start to arise due to not having enough ES to supply the high-power ramp rate load demand. The 25MJ case presents an even more drastic effect to the generators.

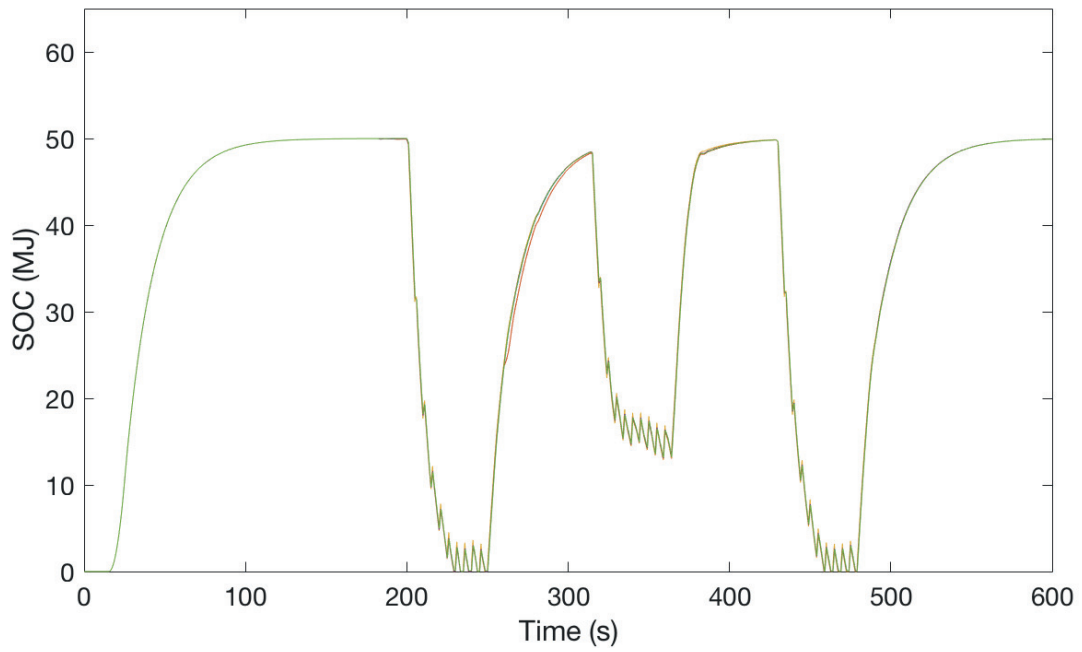


Figure 9. 50MJ 1MW/s ES SOC

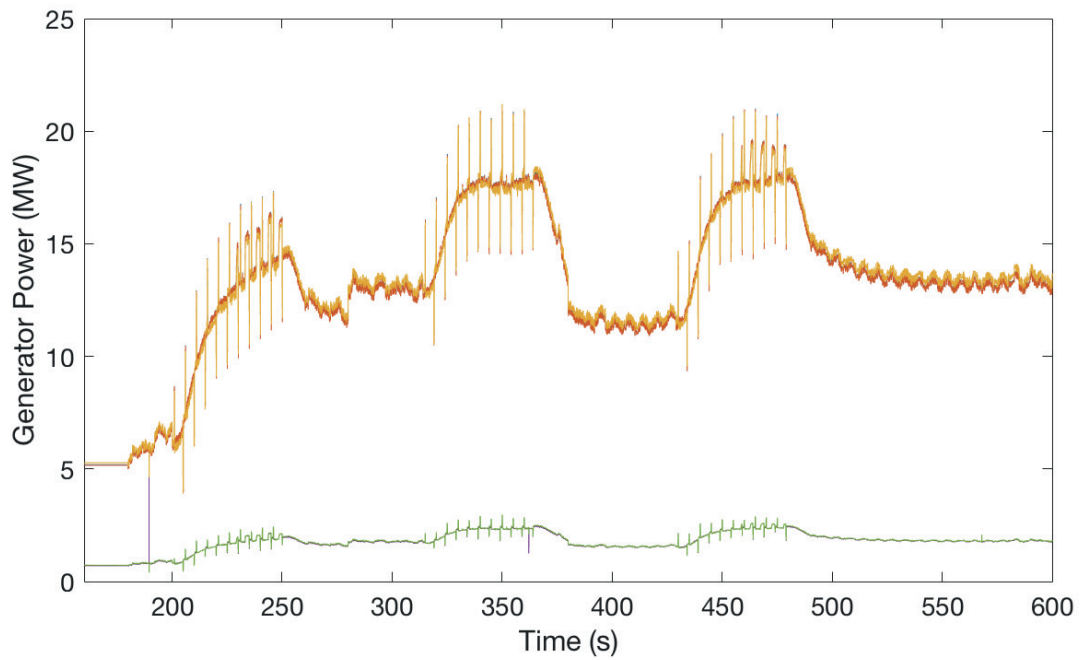


Figure 10. 50MJ 1MW/s Gen Power

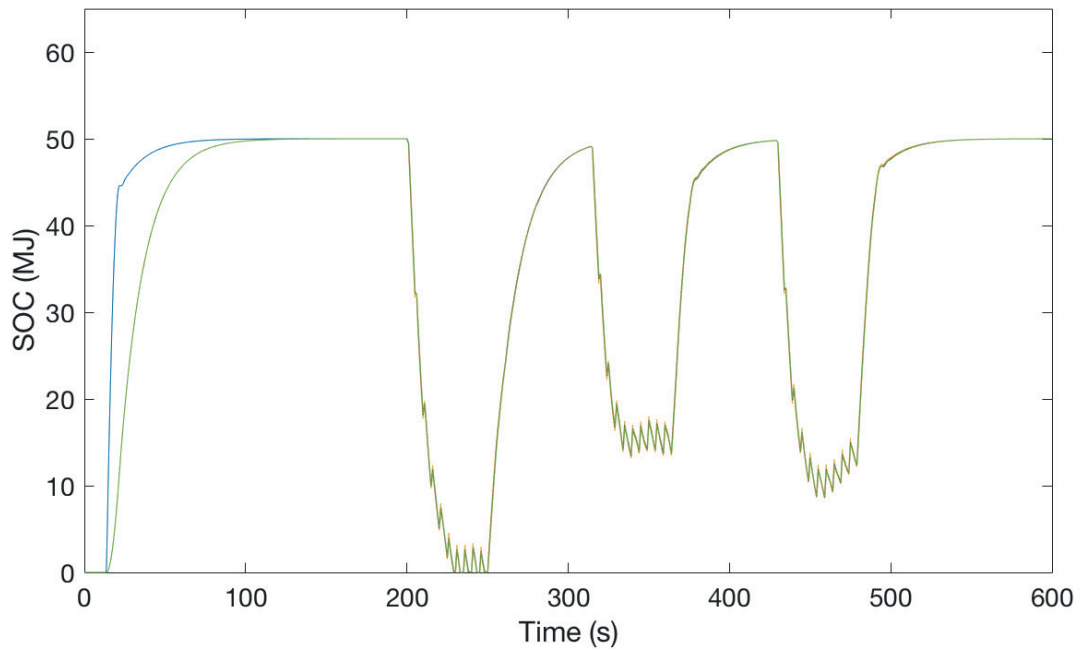


Figure 11. 50MJ 2MW/s ES SOC

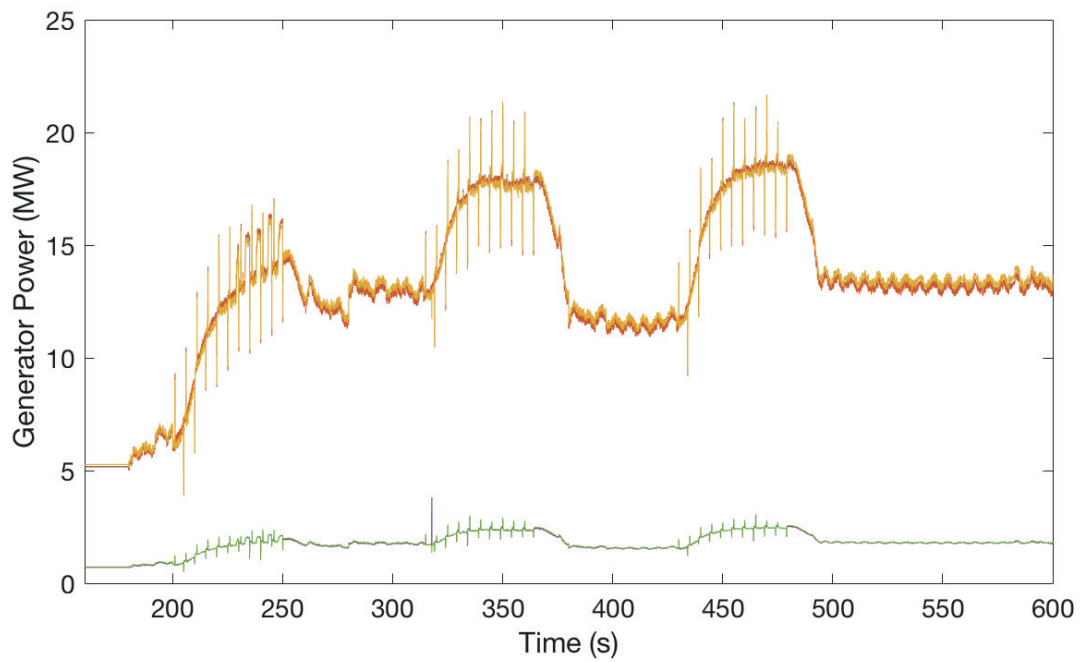


Figure 12. 50MJ 2MW/s Gen Power

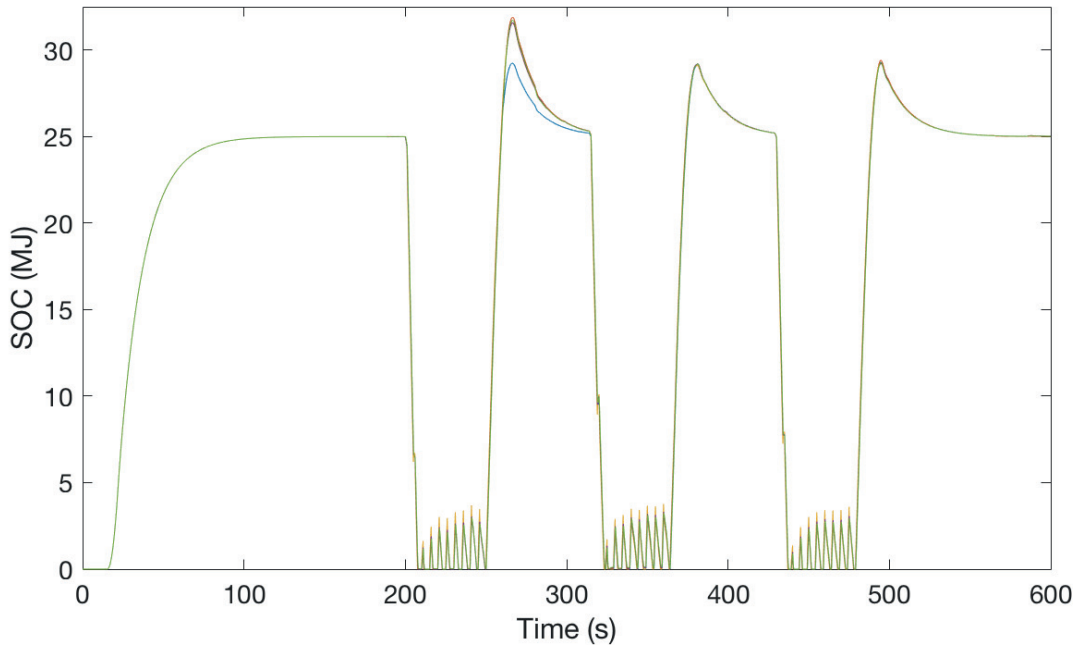


Figure 13. 25MJ 1MW/s ES SOC

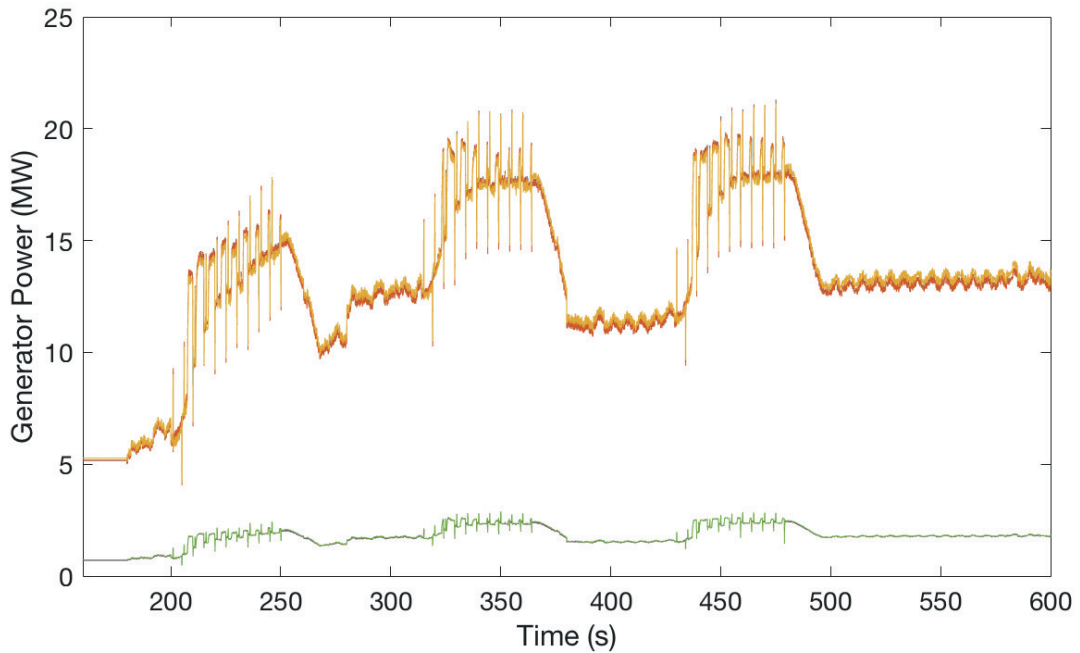


Figure 14. 25MJ 1MW/s Gen Power

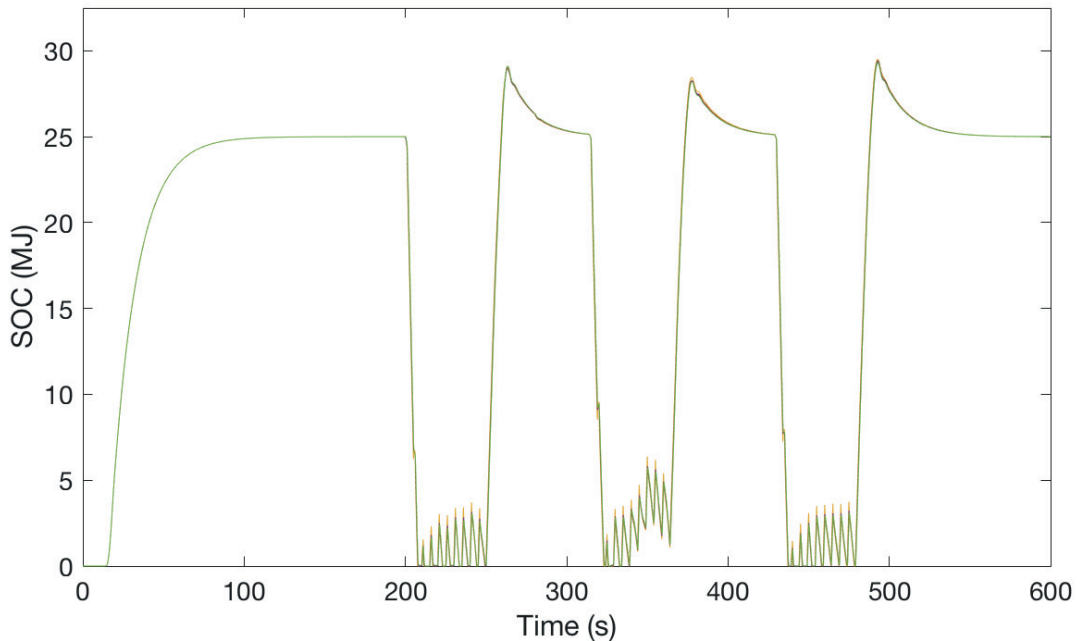


Figure 15. 25MJ 2MW/s ES SOC

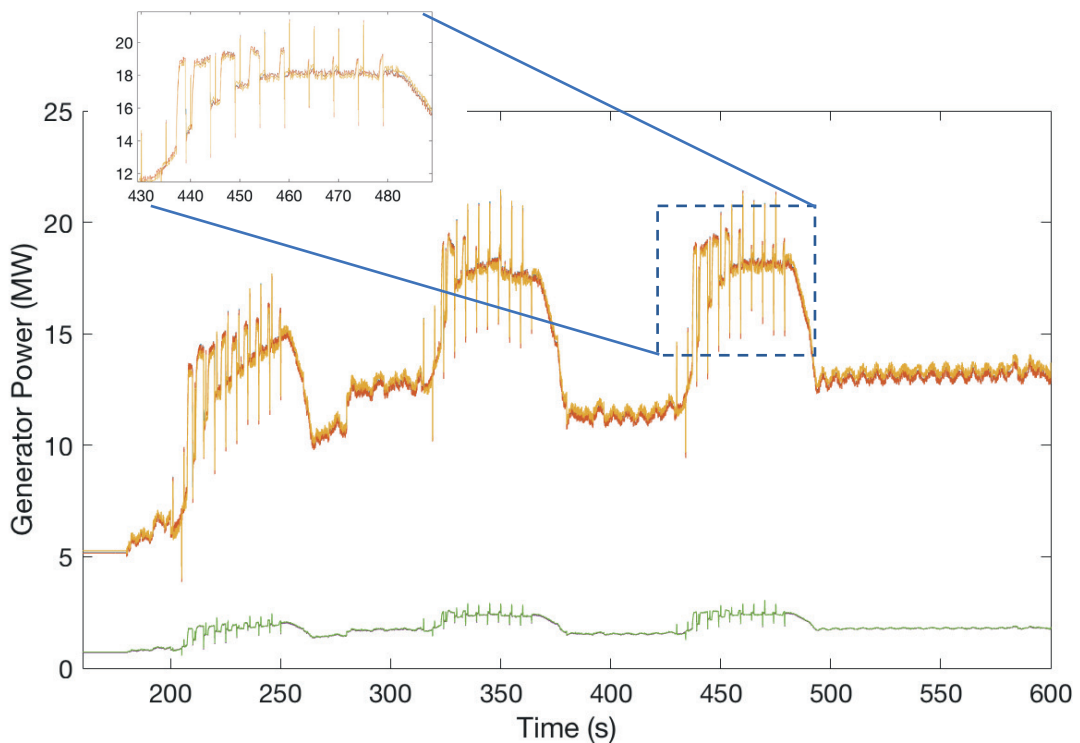


Figure 16. 25MJ 2MW/s Gen Power

The results above show a few interesting points. First of all, for the control used here, the amount of ES is vital to how the generators react to high-power ramp rate loads. Since a spinning reserve control is used when the battle mode is active, the ramp rate of the generators is not taken into account; the ES simply combine to attempt to provide nearly the entire amount of power for the high-power ramp rate load as long as the ES have energy available. Secondly, since the ramp rate is controlled by this EM when the ES are charging, the ramp rate variations for the DMPC with ADMM will only allow the ES to charge faster. This would be beneficial when the system is

in between the group of ten firings. By charging the ES faster, the group of ten firings could potentially be placed closer together, yielding more firings over a span of time if needed.

When looking at the results for 70MJ, 50MJ, and 25MJ, there seem to be some variances with regards to reaching the desired energy reference. By simply changing the energy reference or the ramp rate constraints, an effect can be seen in the control that is not necessarily wanted; over shoot or under shoot can start occurring in a more pronounced manner. This is due to the MPC control not being “tuned” for these particular references and constraints. Finding a good prediction horizon will have quite a large effect on the performance of the control.

As the size of the ES decreased, a noticeable effect on the power output of the generators can be seen. Once the ES SOC are at 0%, the generators must provide the power to service the high-power ramp rate load. For the worst case, 25MJ per ES, it is shown that the first firing depletes the entire energy reserve of the ES. Once the generators’ power output increases, the ES need to provide less power which, in turn, allows the ramp rate of the generators to decrease for the firings. This can be seen in Figure 16.

## 5. Conclusion

Based off of the methodology presented, the amount of ES directly affects what the generators see for high-power ramp rate loads. Having enough ES to supply the high-power ramp rate load for the required time/amount of firings is essential if the generators are to see a minimal power and ramp rate effect. Varying the ramp rate can prove beneficial in the specific circumstance of needing more firings in a smaller amount of time. Increasing the generator ramp rate during the charging stage, which used the DMPC with ADMM, will allow the ES to charge faster.

## 6. Acknowledgements

This material is based upon research supported by, or in part by, the U.S. Office of Naval Research under award numbers N00014-16-1-2956 and N00014-14-1-0718.

## 7. References

- [1] Doerry, Norbert. "Next generation integrated power systems (NGIPS) for the future fleet." *IEEE Electric Ship Technologies Symposium*. 2009.
- [2] Vu, Tuyen V., et al. "Predictive control for energy management in ship power systems under high-power ramp rate loads." *IEEE Transactions on Energy Conversion* (2017).
- [3] L. Wang, *Model predictive control system design and implementation using MATLAB*. London: Springer, 2010.
- [4] R. Negenborn and J. Maestre, "Distributed Model Predictive Control: An Overview and Roadmap of Future Research Opportunities", *IEEE Control Systems*, vol. 34, no. 4, pp. 87-97, 2014.
- [5] Boyd, Stephen, et al. "Distributed optimization and statistical learning via the alternating direction method of multipliers." *Foundations and Trends® in Machine Learning* 3.1 (2011): 1-122.
- [6] H. Park, J. Sun, S. Pekarek, P. Stone, D. Opila, R. Meyer, I. Kolmanovsky, and R. DeCarlo, "Real-Time Model Predictive Control for Shipboard Power Management Using the IPA-SQP Approach," *IEEE Transactions on Control Systems Technology*, 2015.
- [7] F. Garcia-Torres, C. Bordons and M. Ridao, "Optimal Economic Schedule for a Network of Microgrids with Hybrid Energy Storage System using Distributed Model Predictive Control", *IEEE Transactions on Industrial Electronics*, pp. 1-1, 2018.